DOI: 10.1002/ejic.201000857

Germa-*closo*-dodecaborate: An Ambident and Flexible Coordinating Ligand

Jörg-Alexander Dimmer[a] and Lars Wesemann*[a]

Keywords: Germanium / Germylenes / Boranes / Coordination chemistry / Iron / Ruthenium

By following a simple one-pot procedure that starts with $FeBr_2$ and triphos [$MeC(CH_2PPh_2)_3$] or the dimer [$Ru_2(\mu\text{-}Cl)_3(triphos)_2$]Cl in reaction with the nucleophile [$Bu_3MeN]_2[GeB_{11}H_{11}$] in acetonitrile, the zwitterionic acetonitrile adducts [$M(GeB_{11}H_{11})(triphos)(MeCN)_2$] [M = Fe (**1**), M = Ru (**2**)] were isolated in good yield. By means of a facile η^1(Ge) to η^3(B–H) rearrangement, **1** and **2** can be converted into [$M(GeB_{11}H_{11})(triphos)$] [M = Fe (**3**), M = Ru (**4**)]. The nucleophilicity of the germanium cluster vertex in the iron derivative **3** is high enough to react with [$Mo(CO)_5(thf)$] to give the bimetallic complex [$(triphos)Fe(GeB_{11}H_{11})(MoCO)_5$] (**5**), which contains an ambident coordinating germaborate moiety. The new compounds have been characterized by single-crystal X-ray diffraction and elemental analysis. Soluble complexes were also investigated by ^{1}H, ^{11}B, and ^{31}P NMR spectroscopy in solution. In the case of the insoluble complex **1**, solid-state ^{31}P NMR spectroscopy was carried out.

Introduction

Germylenes and stannylenes are strong donor ligands and their structural motifs are numerous.[1] We have in our group an ongoing interest in the chemistry of the heavier homologues of the carba-*closo*-dodecaborate cluster. Whereas the carbon-containing borate cluster is known to behave as a weakly coordinating anion in the protonated form $[CB_{11}H_{12}]^-$,[2] the deprotonated cluster $[CB_{11}H_{11}]^{2-}$ and the higher homologues $[EB_{11}H_{11}]^{2-}$ (E = Ge, Sn) serve as versatile ligands in coordination chemistry.[3,4] It has been shown that the dianions $[SnB_{11}H_{11}]^{2-}$ and $[GeB_{11}H_{11}]^{2-}$ act as σ and π donors with a strong *trans* influence; they readily undergo substitution of halides to form stable complexes containing metal–germanium and metal–tin bonds, respectively.[5–8] These heteroborates can be regarded as a strong-donating germylene or stannylene. In the case of the tin nucleophile, we also have found that this heteroborate cluster acts not only as a terminal ligand but also shows a great variety of coordination modes. Examples for μ_2 coordination in the dimeric complex $[Au_2(SnB_{11}H_{11})_2(PPh_3)_2]^{2-}$, μ_3 coordination in $[\{(Et_3P)Au(SnB_{11}H_{11})\}_3]^{3-}$, and μ_4 coordination in $[\{(dppm)Au_2(SnB_{11}H_{11})_2\}_2]^{4-}$ [dppm = 1,1-bis(diphenylphosphanyl)methane] have been described earlier.[9] Another interesting feature of the stannaborate cluster is its ability to coordinate through η^3(B–H) towards transition-metal fragments.[10] This type of coordination mode was established earlier by Libscomb et al. for $[B_{10}H_{10}]^{2-}$ and by Greenwood et al. for $[B_{12}H_{12}]^{2-}$.[11,12]

In this paper we report transition-metal complexes that contain the germanium nucleophile that coordinates through η^3(B–H), and our studies of the remaining nucleophilicity at the germanium site. Furthermore, we have found a reversible rearrangement from η^1(Ge) to η^3(B–H).

Results and Discussion

To realize the η^3(B–H) coordination mode of the germaborate ligand, we followed the successful synthetic procedure of the homologous tin derivatives. Therefore in a one-pot synthesis, a solution of $FeBr_2$ in acetonitrile was treated with triphos [$MeC(CH_2PPh_2)_3$] and subsequent addition of one equivalent of [$Bu_3MeN]_2[GeB_{11}H_{11}$] dissolved in acetonitrile to result in the formation of the zwitterionic complex **1** as a pink precipitate (Scheme 1). The homologous ruthenium complex **2** was synthesized starting with the dimeric ruthenium triphos complex [$Ru_2(\mu\text{-}Cl)_3(triphos)_2$]Cl (Scheme 2).

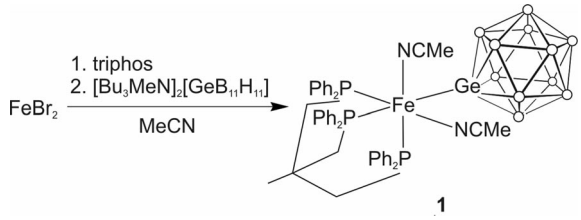

Scheme 1. Formation of the zwitterionic complex [$Fe(GeB_{11}H_{11})(triphos)(MeCN)_2$] (**1**).

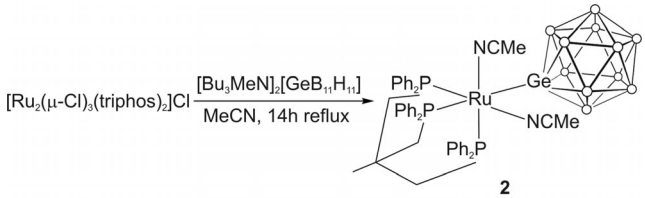

Scheme 2. Formation of the zwitterionic ruthenium complex [$Ru(GeB_{11}H_{11})(triphos)(MeCN)_2$] (**2**).

[a] Institut für Anorganische Chemie, Universität Tübingen,
Auf der Morgenstelle 18, 72076 Tübingen, Germany
Fax: +49-7071-292436
E-mail: lars.wesemann@uni-tuebingen.de

The obtained neutral complexes $[Fe(GeB_{11}H_{11})(triphos)(MeCN)_2]$ and $[Ru(GeB_{11}H_{11})(triphos)(MeCN)_2]$ were insoluble in common solvents and reacted by heating a suspension of **1** in thf or **2** in acetone for several hours under rearrangement of the germa-*closo*-dodecaborate from η^1(Ge) to η^3(B–H) coordination (Scheme 3). Dissolving **3** and **4** in acetonitrile resulted in both cases in the re-formation of the germanium–metal bond to give **1** and **2**.

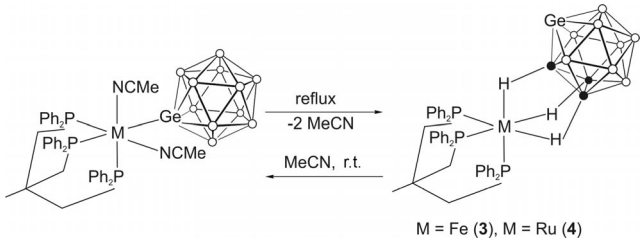

Scheme 3. Rearrangement to give $[Fe(GeB_{11}H_{11})(triphos)]$ (**3**; 9 h reaction time in thf) and $[Ru(GeB_{11}H_{11})(triphos)]$ (**4**; several days' reaction time in acetone). The backreaction: formation of **1** and **2** after one day in acetonitrile.

In the case of the iron derivative **1**, the color of the reaction mixture changed from a red suspension to a dark violet clear solution. For the ruthenium complex **2**, the mixture showed a change from a colorless suspension to a yellow solution. In both η^3(B–H)-coordinated complexes **3** and **4**, the germanium vertex of the heteroborate carries a lone pair. Since these molecules are neutral we were interested in the remaining nucleophilicity at the germaniun(II). Methylation at the germanium is a straightforward reaction with the dianionic borate $[GeB_{11}H_{11}]^{2-}$; however, complex **3** shows no reaction with methyl iodide. Clearly due to complexation at the $[(triphos)Fe]^{2+}$ fragment, the germaborate nucleophilicity was decreased. We also treated iron complex **3** with activated $[Mo(CO)_5(thf)]$ in thf and isolated the bimetallic complex with the germaborate in a bridging coordination mode in a yield of 67% as dark-red-colored crystals (Scheme 4). This type of complex is already known from our investigation of the coordination modes of the homologous tin derivative; in this context we have characterized the series of Cr, Mo, and W complexes $[Fe(SnB_{11}H_{11})(triphos)\{M(CO)_5\}]$ (M = Cr, Mo, W).

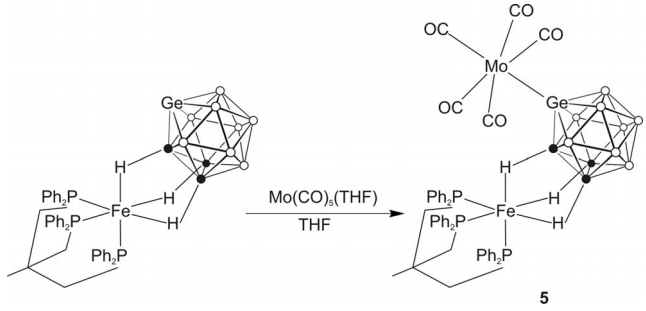

Scheme 4. Synthesis of the binuclear Fe–Mo complex $[Fe(GeB_{11}H_{11})(triphos)(MoCO)_5]$ (**5**).

The new germaborate coordination compounds were characterized by elemental analysis, X-ray crystal-structure analysis, and NMR spectroscopy. Crystal and refinement parameters of the crystal-structure determinations of complexes **1**–**5** are listed in Table 1.

Table 1. Crystal and structure refinement parameters of **1**, **2**, **3**, **4**, and **5**.[a]

	1	**2**	**3**	**4**	**5**
Formula	$C_{53}H_{68}B_{11}FeGeN_6P_3$	$C_{53}H_{68}B_{11}GeN_6P_3Ru$	$C_{43}H_{54}B_{11}Cl_4FeGeP_3$	$C_{43}H_{54}B_{11}Cl_4GeP_3Ru$	$C_{48}H_{54}B_{11}Cl_4FeGeMoO_5P_3$
M_r [gmol^{-1}]	1129.46	1174.61	1053.01	1098.23	1289.00
Crystal system	orthorhombic	orthorhombic	monoclinic	monoclinic	triclinic
Space group	$P2_12_12_1$	$P2_12_12_1$	$C2/c$	$C2/c$	$P\bar{1}$
Z	4	4	8	8	2
a [Å]	16.8535(6)	16.8507(10)	28.1842(17)	28.2025(12)	12.0355(8)
b [Å]	17.5668(7)	17.7270(7)	20.8919(11)	21.0086(10)	13.0976(10)
c [Å]	19.6168(10)	19.6142(7)	21.6978(14)	22.0182(10)	20.8081(15)
α [°]	90	90	90	90	78.494(6)
β [°]	90	90	127.705(4)	128.044(3)	78.049(6)
γ [°]	90	90	90	90	70.182(6)
V [Å^3]	5807.8(4)	5859.0(5)	10108.1(10)	10274.0(8)	2989.0(4)
$\rho_{calcd.}$ [gcm^{-3}]	1.292	1.332	1.384	1.420	1.432
μ [mm^{-1}]	0.891	0.894	1.220	1.212	1.247
F(000)	2344	2416	4304	4448	1300
Crystal size [mm]	0.27×0.26×0.21	0.21×0.17×0.12	2.6×1.5×1.5	0.21×0.19×0.15	0.22×0.21×0.15
θ range [°]	5.69–25.35	5.69–25.35	5.68–25.35	5.68–25.35	5.67–25.35
Limiting indices	$-18 \le h \le 20$	$-20 \le h \le 20$	$-33 \le h \le 33$	$-33 \le h \le 33$	$-14 \le h \le 14$
	$-21 \le k \le 21$	$-21 \le k \le 21$	$-25 \le k \le 25$	$-25 \le k \le 25$	$-15 \le k \le 15$
	$23 \le l \le 23$	$23 \le l \le 23$	$26 \le l \le 25$	$26 \le l \le 26$	$25 \le l \le 25$
Reflections collected	75130	70439	54003	66096	37667
Independent reflections (R_{int})	10515/0.1023	10611/0.1198	9057/0.1284	9308/0.0809	10813/0.0830
Completeness	98.5	98.5	97.9	98.8	98.8
Absorption correction	numerical	numerical	numerical	numerical	numerical
Max./min. transmission	0.9158 and 0.7785	0.9272 and 0.7943	0.8868 and 0.7541	0.8770 and 0.7298	0.8596 and 0.7453
Restraints/parameters	0/622	0/630	0/560	2/569	0/686
R_1/wR_2 [$I > 2\sigma(I)$]	0.0474/0.1081	0.0511/0.1034	0.0759/0.1578	0.0637/0.1327	0.0510/0.1210
R_1/wR_2 for all data	0.0534/0.1108	0.0603/0.1071	0.1033/0.1707	0.0715/0.1368	0.0594/0.1264
GOF on F^2	1.101	1.129	1.076	1.146	1.040
Largest diff. peak/hole [eA^{-3}]	0.952/–0.486	0.509/–0.647	1.444/–1.086	1.682/–1.340	1.108/–0.964
Absolute structure parameter	0.020(10)	0.114(13)	–	–	–

[a] For all cases: λ = 0.71073 Å and T = 173(2) K.

Red crystals of the acetonitrile adduct **1** could be obtained after several days by carefully layering a solution of an equimolar mixture of $FeBr_2$ and triphos in acetonitrile with a solution of one equivalent $[Bu_3MeN]_2[GeB_{11}H_{11}]$ in the same amount of acetonitrile. The zwitterionic complex crystallizes in the orthorhombic space group $P2_12_12_1$ with four molecules of acetonitrile in the asymmetric unit. The molecular structure of the octahedrally coordinated iron complex is depicted in Figure 1 together with selected interatomic distances and bond angles. The interatomic distance between the iron and germanium atom of 2.4575(6) Å is, in relation to values found in the literature, a rather long interatomic distance between iron and germanium.[11,13]

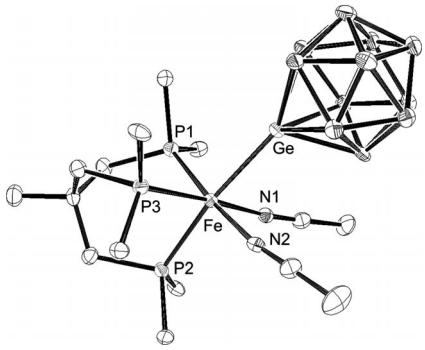

Figure 1. ORTEP plot of $[Fe(GeB_{11}H_{11})(triphos)(MeCN)_2]$ (**1**): The hydrogen atoms and the carbon atoms of the phenyl rings except the *ipso*-carbon atoms have been omitted for clarity; ellipsoids at 50% probability. Interatomic distances [Å] and angles [°]: Fe–Ge 2.4575(6), Fe–P1 2.2530(11), Fe–P2 2.2783(11), Fe–P3 2.2873(11), Fe–N1 1.931(3), Fe–N2 1.941(4); N1–Fe–N2 83.70(14), N1–Fe–P1 91.33(10), N2–Fe–P1 173.38(10), N1–Fe–P2 92.41(10), N2–Fe–P2 95.02(10), P1–Fe–P2 89.53(4), N1–Fe–P3 176.74(10), N2–Fe–P3 93.77(10), P1–Fe–P3 91.35(4), P2–Fe–P3 85.76(4), N1–Fe–Ge 80.59(10), N2–Fe–Ge 80.87(10), P1–Fe–Ge 94.04(3), P2–Fe–Ge 172.20(4), P3–Fe–Ge 101.08(3).

Colorless crystals of **2** were obtained by slow evaporation of the filtered reaction mixture in air. The Ru complex also crystallizes in the orthorhombic space group $P2_12_12_1$ and contains four molecules of acetonitrile in the asymmetric unit. The molecular structure of the zwitterion **2** together with selected interatomic distances and bond angles is depicted in Figure 2. The Ru–Ge distance of 2.5239(6) Å is long in relation to the Ru–Ge distances in the literature (2.403–2.550 Å).[14] The metal phosphorus separations in complexes **1** and **2** are in close range and do not show any significant elongation due to the different ligands in the *trans* position.

Dark violet crystals of the iron complex **3** were obtained by layering a solution of **3** in dichloromethane with hexane. The iron complex crystallizes in the monoclinic space group *C*2/*c* and contains two molecules of dichloromethane in the asymmetric unit. The molecular structure of the neutral complex **3** together with selected interatomic distances and bond angles is shown in Figure 3. The iron–boron separations lie in the close range of 2.2435(1) and 2.2652(1) Å for the coordinated B–H functions.[10d] Compared to the reported analogous tin complex, which shows a rotational disordered cluster fragment, in the case of the germanium cluster, no disorder was detected during the structure refinement.[10d]

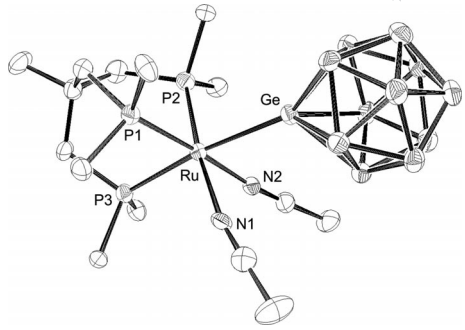

Figure 2. ORTEP plot of $[Ru(GeB_{11}H_{11})(triphos)(MeCN)_2]$ (**2**): The hydrogen atoms and the carbon atoms of the phenyl rings except the *ipso*-carbon atoms have been omitted for clarity; ellipsoids at 50% probability. Interatomic distances [Å] and angles [°]: Ru–N2 2.070(4), Ru–N1 2.095(4), Ru–P2 2.2989(14), Ru–P1 2.3251(14), Ru–P3 2.3456(13), Ru–Ge 2.5239(6); N2–Ru–N1 82.24(17), N2–Ru–P2 92.21(12), N1–Ru–P2 173.02(12), N2–Ru–P1 177.05(12), N1–Ru–P1 95.65(13), P2–Ru–P1 90.05(5), N2–Ru–P3 93.69(11), N1–Ru–P3 95.97(12), P2–Ru–P3 88.58(5), P1–Ru–P3 84.47(5), N2–Ru–Ge 79.73(11), N1–Ru–Ge 80.23(11), P2–Ru–Ge 94.66(4), P1–Ru–Ge 101.98(4), P3–Ru–Ge 172.76(4).

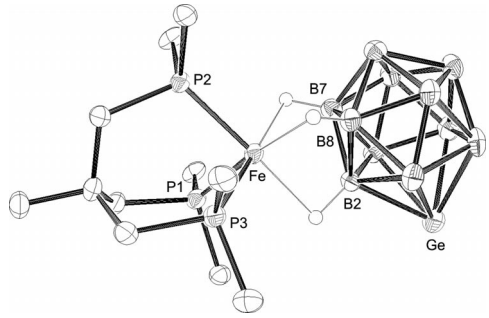

Figure 3. ORTEP plot of $[Fe(GeB_{11}H_{11})(triphos)]$ (**3**): The hydrogen atoms and the carbon atoms of the phenyl rings except the *ipso*-carbon atoms have been omitted for clarity; ellipsoids at 50% probability. Interatomic distances [Å] and angles [°]: Fe–B2 2.2652(1), Fe–B7 2.2571(1), Fe–B8 2.2435(1), Fe–P1 2.2146(16), Fe–P2 2.2043(15), Fe–P3 2.2110(15); P2–Fe–P3 90.22(6), P2–Fe–P1 90.52(6), P3–Fe–P1 90.83(6).

Yellow crystals of the zwitterionic ruthenium complex **4** suitable for X-ray diffraction analysis were obtained by carefully layering a solution of the ruthenium complex in dichloromethane with hexane. Two molecules of dichloromethane could be found in the asymmetric unit, and the complex crystallizes in the monoclinic space group *C*2/*c*. The molecular structure together with selected distances and angles is depicted in Figure 4. Unlike the homologous tin complex of **4**, which shows a disorder between two positions of the cluster with occupancies of 91.1:8.9,[10c] complex **4** exhibits no disorder of the borate. However, the ruthenium–boron distances are between 2.3770(1) and 2.3915(1) Å for B2, B7, and B8, and are comparable with the values found in the tin derivative.[10c]

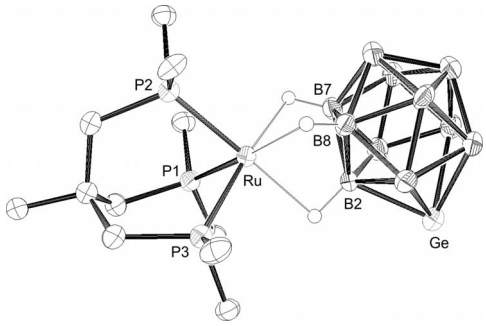

Figure 4. ORTEP plot of [Ru($GeB_{11}H_{11}$)(triphos)] (**4**): The hydrogen atoms and the carbon atoms of the phenyl rings except for the *ipso*-carbon atoms have been omitted for clarity; ellipsoids at 50% probability. Interatomic distances [Å] and angles [°]: Ru–P2 2.2706(12), Ru–P1 2.2723(12), Ru–P3 2.2774(12), Ru–B2 2.3838(1), Ru–B7 2.3770(1), Ru–B8 2.3915(1); P2–Ru–P1 88.17(4), P2–Ru–P3 89.12(4), P1–Ru–P3 89.17(5).

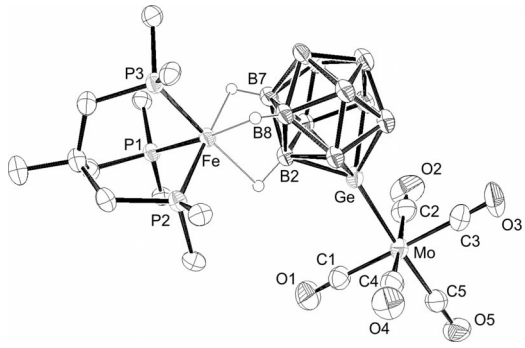

Figure 5. ORTEP plot of [Fe($GeB_{11}H_{11}$)(triphos)($MoCO)_5$] (**5**): The hydrogen atoms and the carbon atoms of the phenyl rings except the *ipso*-carbon atoms have been omitted for clarity; ellipsoids at 50% probability. Interatomic distances [Å] and angles [°]: Fe–B7 2.2575(2), Fe–B2 2.2978(2), Fe–B8 2.2283(1), Mo–C5 1.994(5), Mo–C4 2.036(5), Mo–C3 2.035(5), Mo–C1 2.039(5), Mo–C2 2.040(5), Mo–Ge 2.5758(6), Fe–P3 2.2074(11), Fe–P2 2.2080(10), Fe–P1 2.2275(10), O1–C1 1.137(6), C3–O3 1.136(6), O5–C5 1.143(5), O2–C2 1.135(6), O4–C4 1.137(6); C5–Mo–C4 92.30(19), C5–Mo–C3 90.7(2), C4–Mo–C3 88.3(2), C5–Mo–C1 90.96(19), C4–Mo–C1 90.59(19), C3–Mo–C1 177.98(19), C5–Mo–C2 93.51(19), C4–Mo–C2 173.79(19), C3–Mo–C2 89.5(2), C1–Mo–C2 91.5(2), C5–Mo–Ge 176.13(14), C4–Mo–Ge 86.70(13), C3–Mo–Ge 85.49(14), C1–Mo–Ge 92.78(13), C2–Mo–Ge 87.36(13), P3–Fe–P2 89.81(4), P3–Fe–P1 90.70(4), P2–Fe–P1 90.65(4).

Dark red crystals suitable for single-crystal diffraction could be obtained by carefully layering a solution of **5** in dichloromethane with hexane. The bimetallic complex **5** crystallizes in the triclinic space group $P\bar{1}$ with two molecules of dichloromethane in the asymmetric unit. The molecular structure together with selected interatomic distances and bond angles is depicted in Figure 5. The slight shortening of the molybdenum–carbon bond Mo–C5 [1.994(5) Å] in the *trans* position to the germanium ligand reflects the donor abilities of the heteroborate, thus resulting in π backdonation from the molybdenum to the C5O5 moiety. This small effect is also visible in a small elongation of the C5–O5 bond [1.143(5) Å] and might be compared to [Mo($CO)_5$(PMe_3)] with M–C and C–O bond lengths of 1.984(3) and 1.152(3) Å, respectively.[15] The interatomic distance between the molybdenum and germanium atom of 2.5758(6) Å is comparable to bond lengths reported in the literature.[16]

Because of the insolubility of the zwitterion **1** in common solvents, we conducted solid-state ^{31}P NMR spectroscopic analysis. The spectrum shows three signals at δ = 45.1, 28.4, and 15.9 ppm for the crystalline material due to the missing C_s symmetry in the solid state, thereby resulting in three different ^{31}P nuclei. The solubility of **3** in dichloromethane is moderate but we were still able to conduct multinuclear NMR spectroscopy. Due to the reduced symmetry of **3** relative to the uncoordinated cluster, the $^{11}B\{^1H\}$ NMR spectrum shows seven signals for seven groups of different boron atoms at δ = 0.8, –4.8, –7.0, –12.7, –14.3, –24.1, and –24.8 ppm. In the hydridic region of the $^1H\{^{11}B\}$ NMR spectrum, two broad signals occur with a ratio of 1:2 at δ = –9.71 and –9.94 ppm, thereby reflecting the η^3(B–H) coordination of the cluster fragment at the transition-metal center. Because of the broad signals, it was not possible to detect $^{31}P,^1H$ coupling. The $^{31}P\{^1H\}$ NMR spectrum of **3** shows at low temperatures a typical A_2B pattern, and a $^{31}P,^{31}P$ coupling constant of 57.1 Hz could be determined. The $^1H\{^{11}B\}$ NMR spectrum of **4** shows two doublets at δ = –4.7 and –5.0 ppm in a 2:1 ratio with the respective $^{31}P,^1H$ coupling constants of 28.9 and 36.1 Hz for the *trans* $^{31}P,^1H$ coupling. The *cis* coupling is not resolved due to the broad signals. In the $^{31}P\{^1H\}$ NMR spectrum, a doublet and a triplet with ratio of 2:1 for two different phosphorus atoms were detected. The $^{31}P,^{31}P$ coupling constant could be determined to be 36.8 Hz. In the $^{11}B\{^1H\}$ NMR spectrum six signals were detected at δ = –0.6, –4.6, –6.6, –13.7, –19.9, and –21.0 ppm. The $^{31}P\{^1H\}$ NMR spectrum of the bimetallic complex **5** shows an A_2B pattern at room temperature with a coupling constant of 57.4 Hz for the $^2J(^{31}P,^{31}P)$ coupling, which is very close to the value found for **3**. The $^{11}B\{^1H\}$ NMR spectrum reveals five signals at δ = –2.8, –7.4, –14.8, –25.5, and –27.8 ppm. The signals at δ = –25.5 (2 B) and –27.8 ppm (1 B) belong to the boron atoms with coordination of the B–H units to the iron atom. In these cases, we were able to determine the $^1J(^{11}B,^1H)$ coupling constants to be 85 and 91 Hz. As expected, these values are reduced relative to the uncoordinated B–H units (124–126 Hz) due to coordination at the iron center. Unfortunately, the other boron signals in **3**, **4**, and **5** are very broad, and the respective $^1J(^{11}B,^1H)$ coupling constants could not be resolved. The $^1H\{^{11}B\}$ NMR spectrum of **5** only shows one broad multiplet for the 3 H atoms coordinated to the iron center at δ = –9.8 ppm.

The pentacarbonylmolybdenum complex **5** was also characterized by IR spectroscopy in the solid state. With respect to the molybdenum metal fragment, we found C_{4v} symmetry that resulted in four absorptions in the carbonyl region of the IR spectrum: 2063, 1985, 1926, and 1904 cm^{-1}. These bands can be compared with the germanium trichloride complex $[(CO)_5MoGeCl_3]^-$ that exhibited signals at 2068, 1985, and 1946 cm^{-1}.[17] For the above-mentioned [Mo($CO)_5$(PMe_3)], the corresponding absorptions are located at 2071, 1952, and 1945 cm^{-1}.[18]

Conclusion

As in the case of the homologous tin ligand $[SnB_{11}H_{11}]^{2-}$, the germaborate $[GeB_{11}H_{11}]^{2-}$ shows reversible η^1(Ge) to η^3(B–H) rearrangement when coordinated at [(triphos)Fe]$^{2+}$ or [(triphos)Ru]$^{2+}$ fragments. Coordinated by means of the η^3(B–H) coordination mode at the iron fragment, the germaborate is still nucleophilic enough to show complexation at a $[Mo(CO)_5]$ fragment but shows no reaction with methyl iodide. The found reactivity is completely comparable with the homologous tin chemistry.

Experimental Section

General: All manipulations were carried out under exclusion of air and moisture in an argon atmosphere using standard Schlenk techniques. Solvents were purified by standard methods and stored under argon. Elemental analyses were performed by the Institut für Anorganische Chemie Universität Tübingen with a Vario EL analyzer and a Vario MICRO EL analyzer. The starting material $[Ru_2(\mu\text{-}Cl)_3(triphos)_2]Cl$ was synthesized by the published method.[19] $[Bu_3MeN]_2[GeB_{11}H_{11}]$ was synthesized by a modified protocol of the work of Todd et al.[20] All further chemicals used were purchased commercially and were not further purified.

NMR Spectroscopy: NMR spectra were recorded with a Bruker DRX-250 NMR spectrometer equipped with a 5 mm ATM probe head and operating at 250.13 (^{1}H), 80.25 (^{11}B), and 101.25 MHz (^{31}P) and a Bruker AV-500 NMR spectrometer equipped with a 5 mm ATM probe head and operating at 202.46 MHz (^{31}P). Chemical shifts are reported in δ values in ppm relative to external TMS (^{1}H, ^{13}C), $BF_3{\cdot}Et_2O$ (^{11}B), or 85% aqueous H_3PO_4 (^{31}P) by using the chemical shift of the solvent ^{2}H resonance frequency. The solid-state NMR spectrum of **1** was measured with a Bruker DSX-200 NMR spectrometer operating at 200.13 (^{1}H) and 81.01 MHz (^{31}P). The sample was spinning about the magic angle at 8 kHz in a 4 mm (outside diameter) zirconia rotor. The ^{31}P NMR spectrum was obtained after variable-amplitude cross-polarization (RAMP) from protons and under high-power ^{1}H decoupling. The chemical shift is referenced with respect to external 85% aqueous H_3PO_4(^{31}P) using external ammonium dihydrogen phosphate, 0.81 ppm, as secondary chemical-shift reference. Errors in chemical shifts are estimated to be 0.5 ppm.

Crystallography: X-ray data for compounds **1**–**5** were collected with a Stoe IPDS 2T diffractometer and corrected for Lorentz and polarization effects and absorption by air (Table 1). The programs used in this work were Stoe's X-Area and WinGX suite of programs including SHELXS and SHELXL for structure solution and refinement.[21–26] Numerical absorption correction based on crystal-shape optimization was applied for **1**–**5** with Stoe's X-Red and X-Shape.

CCDC-787319 (for **1**), -787320 (for **2**), -787318 (for **3**), -787321 (for **4**), and -787322 (for **5**) contain the supplementary crystallographic data for this paper. These data can be obtained free of charge from The Cambridge Crystallographic Data Centre via www.ccdc.cam.ac.uk/data_request/cif.

[1-{Fe(MeCN)$_2$(triphos)}-GeB$_{11}$H$_{11}$]·4MeCN (1): All hydrogen atoms were placed in calculated positions and refined with isotropic thermal parameters. All solvate acetonitrile molecules were refined isotropically.

[1-{Ru(MeCN)$_2$(triphos)}-GeB$_{11}$H$_{11}$]·4MeCN (2): All hydrogen atoms were placed in calculated positions and refined with isotropic thermal parameters. All solvate acetonitrile molecules were refined isotropically. The acetonitrile C61–C60–N6/C61–C70–N7 is disordered over two positions.

[2,7,8-(μ-H)$_3$-{Fe(triphos)}-GeB$_{11}$H$_{11}$]·2CH$_2$Cl$_2$ (3): All hydrogen atoms were placed in calculated positions and refined with isotropic thermal parameters. All solvate dichloromethane molecules show disorder and were refined isotropically.

[2,7,8-(μ-H)$_3$-{Ru(triphos)}-GeB$_{11}$H$_{11}$]·2CH$_2$Cl$_2$ (4): All hydrogen atoms were placed in calculated positions and refined with isotropic thermal parameters. Two DFIX restraints were applied for the dichloromethane molecule C10–Cl1/Cl2.

[1-{Mo(CO)$_5$}-2,7,8-(μ-H)$_3$-{Fe(triphos)}-GeB$_{11}$H$_{11}$]·2CH$_2$Cl$_2$ (5): All hydrogen atoms were placed in calculated positions and refined with isotropic thermal parameters. The dichloromethane molecule C30–Cl3/Cl4; C50–Cl3/Cl5 is disordered over two positions.

[1-{Fe(MeCN)$_2$(triphos)}-GeB$_{11}$H$_{11}$] (1): $FeBr_2$ (0.16 mmol, 35 mg) was dissolved in acetonitrile (10 mL). Afterwards, triphos (0.16 mmol, 100 mg) was added as a solid. The color of the solution changed to intense red. After stirring for 20 min, $[Bu_3MeN]_2[GeB_{11}H_{11}]$ (0.16 mmol, 100 mg) in acetonitrile (10 mL) was added with a syringe and a pink precipitate formed immediately. That was filtered off and washed with acetonitrile (3 × 5 mL). The solid (123 mg, 80% yield) was dried under reduced pressure. Red crystals of **1** were obtained after several days by layering a filtered mixture of $FeBr_2$ and triphos with a solution of $[Bu_3MeN]_2[GeB_{11}H_{11}]$ in the same amount of acetonitrile. $C_{45}H_{56}B_{11}FeGeN_2P_3$ (965.25 g mol^{-1}): calcd. C 56.00, H 5.85, N 2.90; found C 55.78, H 6.12, N 2.79.

[1-{Ru(MeCN)$_2$(triphos)}-GeB$_{11}$H$_{11}$] (2): $[Ru_2(\mu\text{-}Cl)_3(triphos)_2]Cl$ (0.08 mmol, 132 mg) was dissolved in acetonitrile (15 mL). $[Bu_3MeN]_2[GeB_{11}H_{11}]$ (0.17 mmol, 100 mg) in acetonitrile (10 mL) was added to the yellow solution, and the solution was heated under reflux for 14 h. The colorless precipitate was filtered off and washed with dichloromethane (2 × 5 mL). The product (94 mg, 56% yield) was dried under reduced pressure. Single crystals could be obtained by slow evaporation from the filtered reaction mixture. $C_{45}H_{56}B_{11}GeN_2P_3Ru$ (1010.48 g mol^{-1}): calcd. C 53.49, H 5.59, N 2.77; found C 53.24, H 5.70, N 2.85.

[2,7,8-(μ-H)$_3$-{Fe(triphos)}-GeB$_{11}$H$_{11}$] (3): Compound **1** (0.10 mmol, 100 mg) was suspended in THF (15 mL) and heated to reflux until a clear violet solution was obtained (about 9 h). The solvent was evaporated under reduced pressure and the crude material was taken up in dichloromethane (15 mL). By layering the filtered solution with hexane, dark violet crystals of **3**·2CH_2Cl_2 (89 mg, 82% yield) were grown. ^{1}H{^{11}B} NMR (CD_2Cl_2, 250.13 MHz): δ = 6.8–7.3 (m, 30 H, C_6H_5), 2.50 (m, 6 H, CH_2), 1.82 (s, 3 H, CH_3), –9.7 (br., 1 H, Fe–H–B), –9.9 (br., 2 H, Fe–H–B) ppm. ^{11}B NMR (CD_2Cl_2; 80.25 MHz): δ = 0.8, –4.8, –7.0, –12.7, –14.3, –24.1, –24.8 (11 B) ppm. ^{31}P{^{1}H} NMR (CD_2Cl_2, –50 °C, 202.46 MHz): δ = 55.1 [m, ^2J(P,P) = 57.1 Hz, 2 P], 54.6 [m, ^2J(P,P) = 57.1 Hz, 1 P] ppm. $C_{41}H_{50}B_{11}FeGeP_3{\cdot}(CH_2Cl_2)_2$ (1053.01 g mol^{-1}): calcd. C 49.05, H 5.17; found C 49.11, H 4.52.

[2,7,8-(μ-H)$_3$-{Ru(triphos)}-GeB$_{11}$H$_{11}$] (4): A suspension of **2** (0.05 mmol, 50 mg) in acetone (30 mL) was heated under reflux for several days. The reaction mixture turned yellow and the unreacted starting material was filtered off the yellow solution. The solvent of the filtrate was removed under reduced pressure, thereby leaving a yellow powder (19 mg, 40% yield) that was dried overnight. The yield could be increased by suspending the unreacted starting material in acetone and again heating under reflux. By layering a solution of the product in dichloromethane with hexane, yellow crystals

of **4** could be obtained. $^1H\{^{11}B\}$ NMR (CD_2Cl_2, 250.13 MHz): δ = 6.8–7.3 (m, 30 H, C_6H_5), 2.53 (m, 6 H, CH_2), 1.78 (s, 3 H, CH_3), –4.7 [d, ^2J(P,H) = 27.4 Hz, 2 H, Ru–H–B], –5.0 [d, ^2J(P,H) = 36.3 Hz, 1 H, Ru–H–B] ppm. ^{11}B NMR (CD_2Cl_2, 80.25 MHz): δ = –0.6, –4.6, –6.6, –13.7, –19.9, –21.0 (11 B) ppm. $^{31}P\{^1H\}$ NMR (CD_2Cl_2, –50 °C, 202.46 MHz): δ = 46.8 [d, ^2J(P,P) = 36.7 Hz, 2 P], 45.4 [t, ^2J(P,P) = 36.9 Hz, 1 P] ppm. $C_{41}H_{50}B_{11}RuGeP_3$ (928.37 g mol^{-1}): calcd. C 53.04, H 5.43; found C 53.07, H 5.48.

[1-{Mo(CO)$_5$}-2,7,8-(μ-H)$_3$-{Fe(triphos)}-GeB$_{11}$H$_{11}$] (5): A solution of [Mo(CO)$_6$] (0.06 mmol, 15 mg) in THF (30 mL) was irradiated for 2 h using a UV lamp. The resulting yellow solution was added at once to [2,7,8-(μ-H)$_3$-{Fe(triphos)}-GeB$_{11}$H$_{11}$] (0.06 mmol, 50 mg) and the dark red solution was stirred for 20 min. The solution was concentrated under reduced pressure to approximately 10 mL and layered with hexane. After several days intense dark red crystals of **5** were obtained (47 mg, 67% yield), collected by filtration, and dried under reduced pressure. Recrystallization from CH_2Cl_2/hexane yielded crystals suitable for X-ray diffraction. IR (ATR): $\tilde{\nu}$ = 2066 [s, CO, $A_1^{(2)}$], 1985 (m, CO, B_1), 1926 (vs, CO, E), 1904 [m, CO, $A_1^{(1)}$] cm^{-1}. $^1H\{^{11}B\}$ NMR (CD_2Cl_2, 250.13): δ = 6.8–7.2 (m, 30 H, C_6H_5), 2.53 (m, 6 H, CH_2), 1.83 (s, 3 H, CH_3), –9.82 (m, 3 H, Fe–*H*–B) ppm. ^{11}B NMR (CD_2Cl_2, 80.25 MHz): δ = –2.8, –7.4, –14.8, –25.5 ($^1J^{11}B$-^1H = 85 Hz), –27.8 ($^1J^{11}B$-^1H = 91 Hz) (11 B) ppm. $^{31}P\{^1H\}$ NMR (CD_2Cl_2, 101.25 MHz): δ = 51.6 [m, ^2J(P,P) = 57.4 Hz, 2 P], 53.4 [m, ^2J(P,P) = 57.4 Hz, 1 P] ppm. $C_{46}H_{50}B_{11}FeGeMoO_5P_3 \cdot 0.5CH_2Cl_2$ (1161.61 g mol^{-1}): calcd. C 48.08, H 4.43; found C 48.08, H 4.45.

Acknowledgments

Financial support from the Deutsche Forschungsgemeinschaft (DFG) is gratefully acknowledged.

[1] a) D. H. Harris, M. F. Lappert, J. B. Pedley, G. J. J. Sharp, *J. Chem. Soc., Dalton Trans.* **1976**, 945–950; b) P. J. Davidson, D. H. Harris, M. F. Lappert, *J. Chem. Soc., Dalton Trans.* **1976**, 2268–2274; c) R. D. Adams, E. Trufan, *Inorg. Chem.* **2010**, *49*, 3029–3034; d) M. Weidenbruch, *Eur. J. Inorg. Chem.* **1999**, 373–381; e) K. W. Klinkhammer, in: *Chemistry of Organic Germanium, Tin and Lead Compounds* (Ed.: Z. Rappoport), Wiley, New York, **2002**, vol. 2, pp. 283–357; f) M. Veith, *Angew. Chem. Int. Ed. Engl.* **1987**, *26*, 1–14; g) J. Barrau, G. Rima, *Coord. Chem. Rev.* **1998**, *178–180*, 593–622; h) N. Tokitoh, R. Okazaki, *Coord. Chem. Rev.* **2000**, *210*, 251–277; i) S. Yao, Y. Xiong, M. Driess, *Chem. Commun.* **2009**, 6466–6468; j) O. Kühl, *Coord. Chem. Rev.* **2004**, *248*, 411–427; k) S. Nagendran, H. W. Roesky, *Organometallics* **2008**, *27*, 457–492; l) S. Inoue, M. Driess, *Organometallics* **2009**, *28*, 5032–5035; m) A. Shinohara, J. McBee, T. D. Tilley, *Inorg. Chem.* **2009**, *48*, 8081–8083; n) A. V. Zabula, F. E. Hahn, *Eur. J. Inorg. Chem.* **2008**, 5165–5179.

[2] For recent reviews, see: a) I. Krossing, I. Raabe, *Angew. Chem.* **2004**, *116*, 2116–2142; b) C. A. Reed, *Chem. Commun.* **2005**, 1669–1677.

[3] M. Finze, J. A. P. Sprenger, *Chem. Eur. J.* **2009**, *15*, 9918–9927.

[4] a) L. Wesemann, T. Marx, U. Englert, M. Ruck, *Eur. J. Inorg. Chem.* **1999**, *9*, 1563–1566; b) T. Marx, B. Mosel, I. Pantenburg, S. Hagen, H. Schulze, L. Wesemann, *Chem. Eur. J.* **2003**, *9*, 4472–4478; c) L. Wesemann, *Z. Anorg. Allg. Chem.* **2004**, *630*, 1349–1356; d) T. Gädt, L. Wesemann, *Organometallics* **2007**, *26*, 2474–2481; e) M. Kirchmann, K. Eichele, F. M. Schappacher, R. Pöttgen, L. Wesemann, *Angew. Chem. Int. Ed.* **2008**, *47*, 963–966.

[5] J.-A. Dimmer, H. Schubert, L. Wesemann, *Chem. Eur. J.* **2009**, *15*, 10613–10619.

[6] M. Kirchmann, T. Gädt, F. M. Schappacher, R. Pöttgen, F. Weigend, L. Wesemann, *Dalton Trans.* **2009**, 1055–1062.

[7] J.-A. Dimmer, M. Hornung, F. Weigend, L. Wesemann, *Dalton Trans.* **2010**, DOI: 10.1039/c003042b.

[8] a) T. Marx, L. Wesemann, S. Dehnen, I. Pantenburg, *Chem. Eur. J.* **2001**, *7*, 3025–3032; b) T. Marx, L. Wesemann, I. Pantenburg, *Organometallics* **2001**, *20*, 5241–5244; c) S. Hagen, T. Marx, I. Pantenburg, L. Wesemann, M. Nobis, B. Drießen-Hölscher, *Eur. J. Inorg. Chem.* **2002**, 2261–2265; d) T. Marx, B. Mosel, I. Pantenburg, S. Hagen, H. Schulze, L. Wesemann, *Chem. Eur. J.* **2003**, *9*, 4472–4478.

[9] a) S. Hagen, I. Pantenburg, F. Weigend, C. Wickleder, L. Wesemann, *Angew. Chem. Int. Ed.* **2003**, *42*, 1501–1505; b) S. Hagen, L. Wesemann, I. Pantenburg, *Chem. Commun.* **2005**, 1013–1015; c) S. Hagen, H. Schubert, C. Maichle-Mössmer, I. Pantenburg, F. Weigend, L. Wesemann, *Inorg. Chem.* **2007**, *46*, 6775–6784; d) H. Schubert, L. Wesemann, *Organometallics* **2010**, DOI: 10.1021/om1001556.

[10] a) T. Gädt, B. Grau, K. Eichele, I. Pantenburg, L. Wesemann, *Chem. Eur. J.* **2006**, *12*, 1036–1045; b) T. Gädt, L. Wesemann, *Dalton Trans.* **2006**, 328–329; c) T. Gädt, K. Eichele, L. Wesemann, *Dalton Trans.* **2006**, 2706–2713; d) T. Gädt, K. Eichele, L. Wesemann, *Organometallics* **2006**, *25*, 3904–3911.

[11] T. E. Paxson, M. F. Hawthorne, L. D. Brown, W. N. Lipscomb, *Inorg. Chem.* **1974**, *13*, 2772–2774.

[12] M. Elrington, N. N. Greenwood, J. D. Kennedy, M. J. Thornton-Pett, *J. Chem. Soc., Dalton Trans.* **1987**, 451–456.

[13] a) H. Tobita, K. Ishiyama, Y. Kawano, S. Inomata, H. Ogino, *Organometallics* **1998**, *17*, 789–794; b) L. W. Pineda, V. Jancik, J. F. Colunga-Valladares, H. W. Roesky, A. Hofmeister, J. Magull, *Organometallics* **2006**, *25*, 2381–2383; c) C. Jones, R. P. Rose, A. Stasch, *Dalton Trans.* **2008**, 2871–2878.

[14] a) R. D. Adams, B. Captain, E. Trufan, *J. Cluster Sci.* **2007**, *18*, 642–659; b) R. Ball, M. J. Bennett, *Inorg. Chem.* **1972**, *11*, 1806–1811; c) L. Y. Y. Chan, W. H. G. Graham, *Inorg. Chem.* **1975**, *14*, 1778–1781; d) B. Marciniec, H. Lawicka, M. Maychrzak, M. Kubicki, I. Kownacki, *Chem. Eur. J.* **2006**, *12*, 244–250.

[15] M. S. Davies, M. J. Aroney, I. E. Buys, T. W. Hambley, J. L. Calvert, *Inorg. Chem.* **1995**, *34*, 330–336.

[16] a) M. Zyder, A. Kochel, T. Szymanska-Buzar, *J. Organomet. Chem.* **2009**, *694*, 4196–4203; b) A. C. Filippou, J. G. Winter, G. Kociok-Kohn, I. Hinz, *J. Organomet. Chem.* **1997**, *542*, 35; c) O. Kühl, P. Lönnecke, J. Heinicke, *Inorg. Chem.* **2003**, *42*, 2836–2828.

[17] J. K. Ruff, *Inorg. Chem.* **1967**, *6*, 1502–1504.

[18] M. S. Davies, R. K. Pierens, M. J. Aroney, *J. Organomet. Chem.* **1993**, *458*, 141–146.

[19] B. D. Yeomans, D. G. Humphrey, G. A. Heath, *J. Chem. Soc., Dalton Trans.* **1997**, 4153–4166.

[20] R. W. Chapman, J. G. Chester, K. Folting, W. E. Streib, L. J. Todd, *Inorg. Chem.* **1992**, *31*, 979–983.

[21] *X-AREA 1.26*, Stoe & Cie GmbH, Darmstadt, Germany, **2004**.

[22] L. F. Farrugia, *J. Appl. Crystallogr.* **1999**, *32*, 837–838.

[23] G. M. Sheldrick, *SHELXS 97*, Program for the Solution of Crystal Structures, Göttingen, Germany, **1997**.

[24] G. M. Sheldrick, *SHELXS 97*, Program of the Crystal Structure Refinement, Göttingen, Germany, **1997**.

[25] *X-RED 1.26*, Data Reduction for STAD4 and IPDS, Stoe & Cie, Darmstadt, **1996**.

[26] *X-SHAPE 2.05*, Crystal optimization for absorption correction, Stoe & Cie, Darmstadt, Germany, **1996**.

Received: August 9, 2010
Published Online: November 4, 2010

